Supplementary Information

Three-Dimensional Porous Metal Phosphide Cathode Electrodes Prepared via Electroless Galvanic Modification for Alkaline Water Electrolysis

Sankar Sasidharan,[1] Rajith Illathvalappil,[1] S. Assa Aravindh,[2] Hidenori Kuroki,[1] Gopinathan M. Anilkumar,[1,3] Takeo Yamaguchi[1]*

[1]Laboratory for Chemistry and Life Science, Tokyo Institute of Technology, R1-17, 4259 Nagatsuta, Midori-ku, Yokohama, Japan 226-8503

*E-mail: yamag@res.titech.ac.jp

[2]Nano and Molecular Systems Research Unit (NANOMO), Pentti Kaiteran katu 1, Linnanmaa, University of Oulu, Oulu- 90014, Finland

[3]R&D Centre, Noritake Co., Ltd., 300 Higashiyama, Miyochi-cho, Miyoshi 470-0293, Japan

Figure S1. Photograph showing the deposition of Ni particles after the galvanic replacement by Ru on the nickel foam (NF) surface after 24 h immersion in $RuCl_3$ solution.

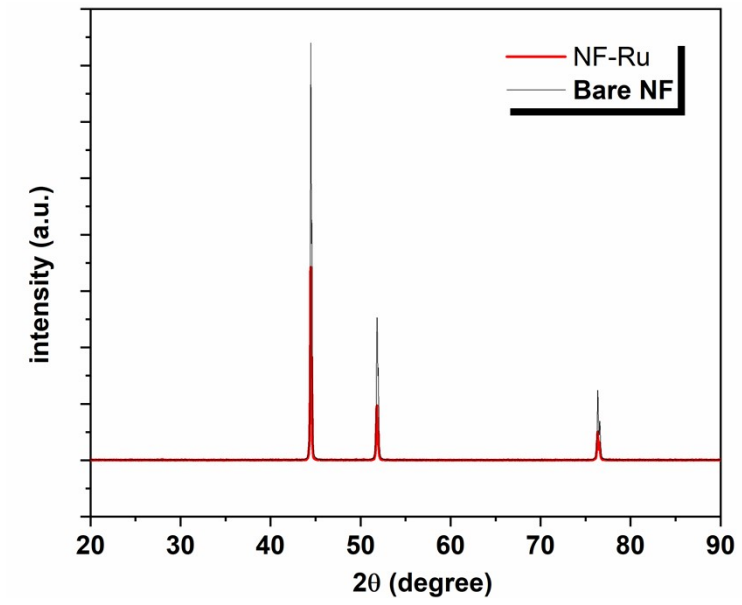

Figure S2. XRD patterns for NF-Ru in comparison with bare NF

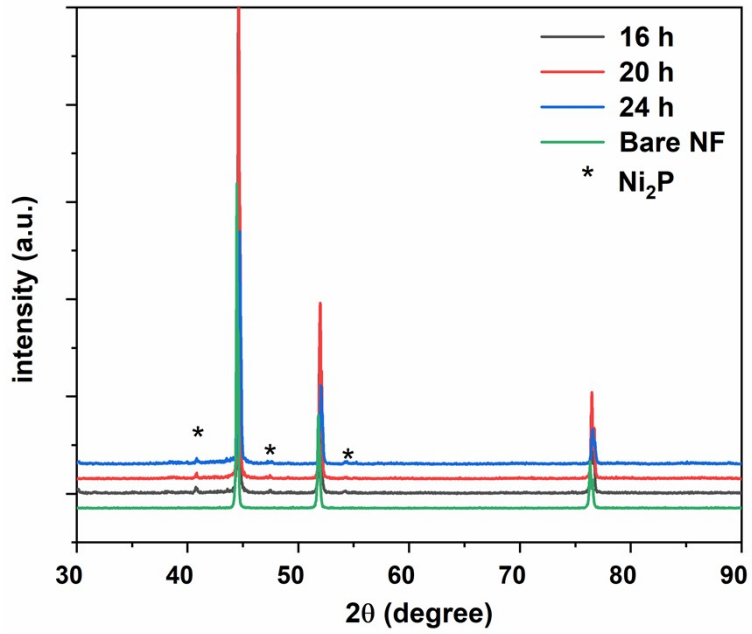

Figure S3. XRD patterns for Ni_2P-Ru/NF developed after keeping the NF in $RuCl_3$ solution at different times (3, 16, 20 and 24 h).

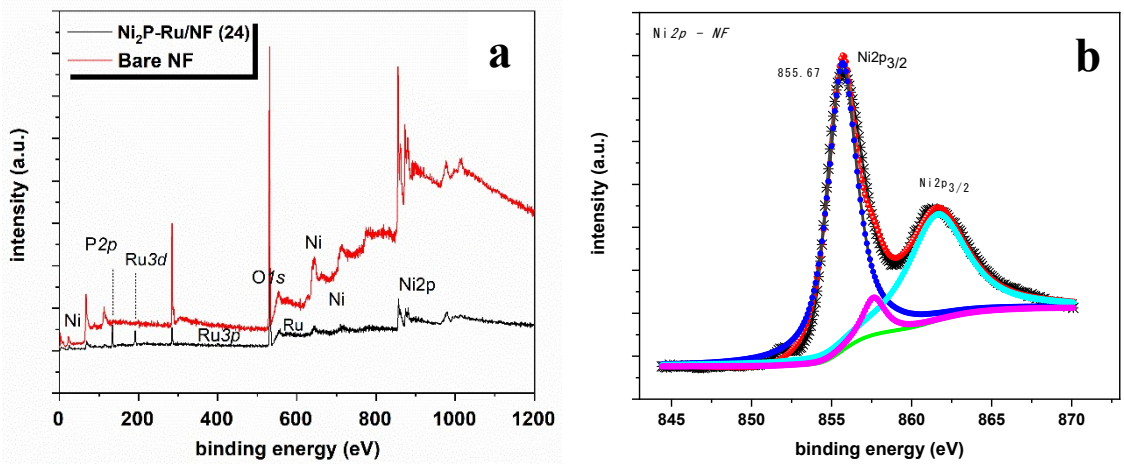

Figure S4. a) XPS survey spectra for Ni_2P-Ru/NF (24 h) and bare NF. **b)** XPS deconvoluted spectrum for Ni *2p* (bare NF).

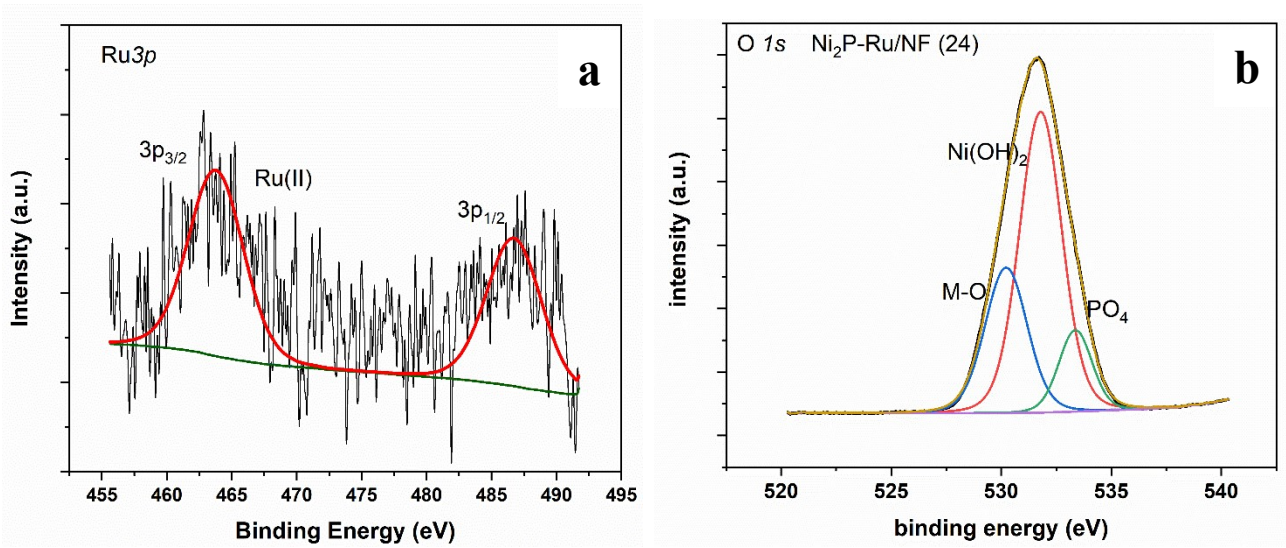

Figure S5. XPS deconvoluted spectra for Ni_2P-Ru/NF (24 h): **a)** Ru *3p* and **b**) O *1s*.

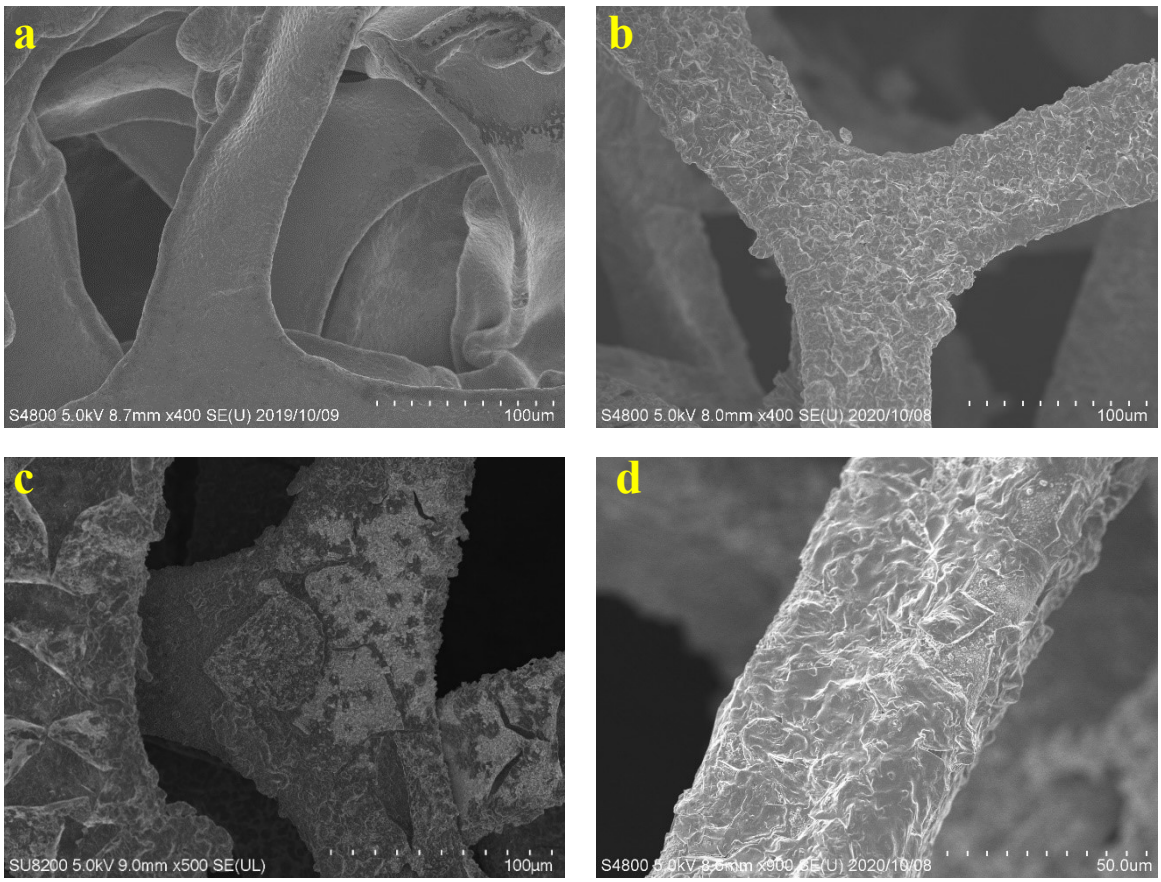

Figure S6. SEM micrographs of **a**) bare NF and **b-d**) Ni_2P-Ru/NF (24 h) catalysts.

Catalyst	Immersion time in $RuCl_3$ solution (h)	Overpotential at 10/20 mA cm^{-2} (mV)
Ni_2P-Ru/NF (3 h)	3	113/145
Ni_2P-Ru/NF (16 h)	16	92/114
Ni_2P-Ru/NF (20 h)	20	69/88
Ni_2P-Ru/NF (24 h)	24	40/60
Bare NF	–	329/364
Ni_2P/NF	–	290/316
Pt-Ru/C	–	23/28

Table S1. HER performance for the different catalysts in the study.

Table S2. Comparison of the alkaline HER performance of Ni_2P-Ru/NF (24 h) with recent literature on Ru- and Ni-based catalysts in 1 M KOH solution.

Catalyst	Current density (mA cm^{-2})	**Overpotential (mV)**	**Reference**
Ni_2P-Ru/NF (24 h)	100	107	Present work
Ni_2P-Ru/NF (24 h)	10	40	Present work
Ru-S-2/C	10	40	1
RuP_2@NPC	10	52	2
Ru@C_2N	10	17	3
RuSi	10	37	4
Ru_2P	10	57	5
Ru-Ru_2P@PC	10	43.4	6
P-Ru/C	10	31	7
S-RuP@NPSC-900	10	92	8
Ru/CoO	10	55	9
Ru_1CoP/CDs-1000	10	51	10
Ru SAs-Ni_2P NPs	10	57	11
$NiRu_{0.13}$-BDC	10^2	34	12
NiCoDPA	10	112	13
Ni-Fe/$NiMoN_x$/NF	20	49	14
NiFeOOH/NF	10	145	15
Ru/Ni_2P/NF	100	130	16
RuCoP/NF	10	44	17
CeO_x-NiB@NF	10	19	18
Co_2Fe-P	10	48	19
Cu_2S/Ni_3S_2/NF-3	10	50	20
CoS_2-2	10	288	21

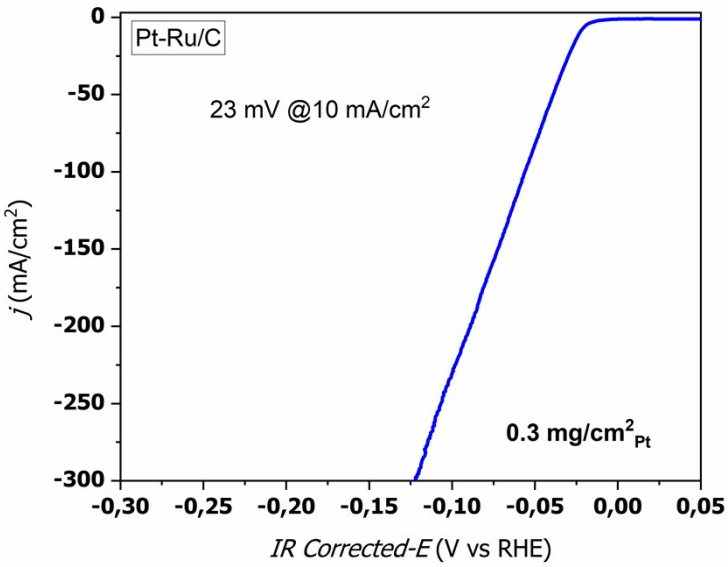

Figure S7. HER curve recorded for PtRu/C in N_2 saturated 1M KOH solution.

Table S3. Comparison of the OWS performance of IrO_2/NF||Ni_2P-Ru/NF with recent reports in 1 M KOH electrolyte solution.

Anode||Cathode	Current density (mA cm^{-2})	**Potential (V)**	**Reference**
IrO_2/NF||Ni_2P-Ru/NF	10	1.6	Present work
RuCoP/NF||RuCoP/NF	10	1.533	21
IrO_2@MnO_2/rGO||IrO_2@MnO_2/rGO	10	1.6	22
NiV/Ir LDH||NiV/Ir LDH	10	1.49	23
IrNi/NF||IrNi/NF	10	1.6	24
Ni-S-Se/NF||Ni-S-Se/NF	10	1.57	25
Ni_2P−CuP_2/NF||Ni_2P−CuP_2/NF	10	1.45	26
NiFeOOH/NF||NiFeOOH/NF	10	1.59	27
LSC/K-$MoSe_2$||LSC/K-$MoSe_2$	10	1.59	28
Co_2Fe-P||Co_2Fe-P	10	1.54	19
Ir_1@Co/NC||Ir_1@Co/NC	10	1.61	29
MnO_2/Co_3O_4||MnO_2/Co_3O_4	10	1.66	30

Ru-Ni_2P/NiO/NF HNSs || S-(Ni,Fe)OOH /NF	50	1.63	31

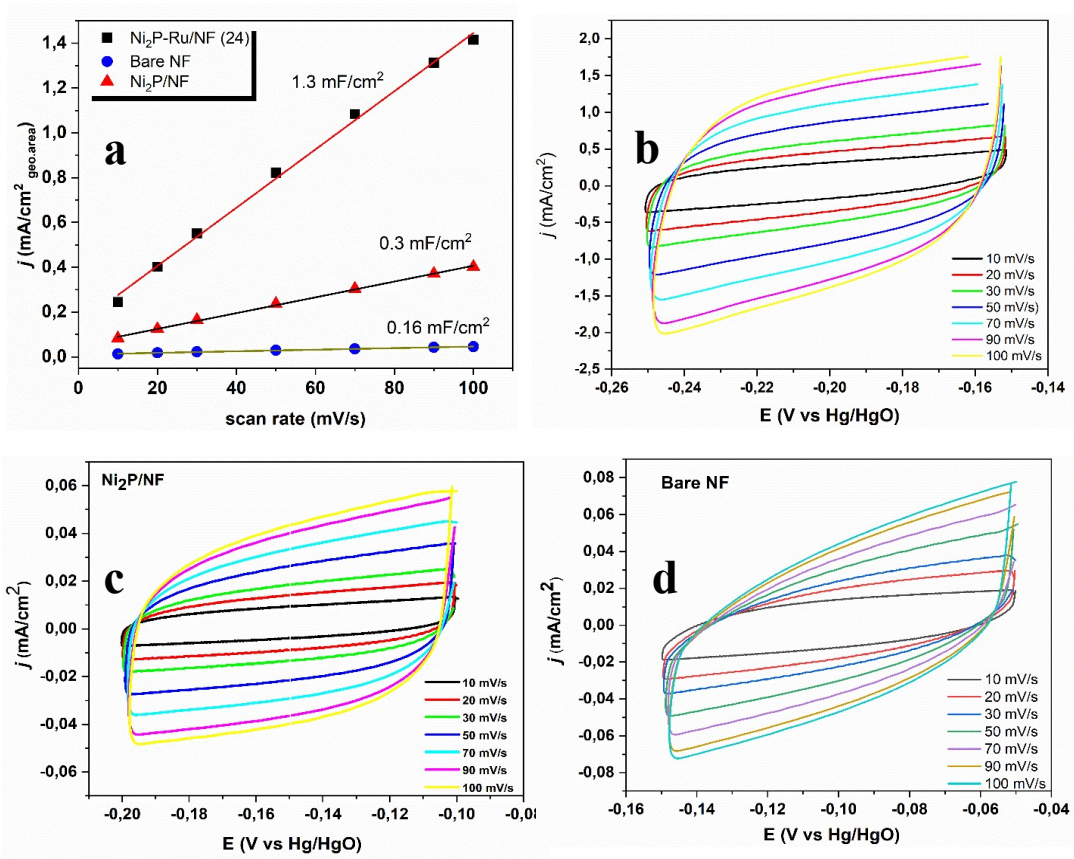

Figure S8. a) Linear fitting of current density vs scan rate showing the C_{dl} for bare NF, Ni_2P/NF and Ni_2P-Ru/NF (24 h) catalysts. CV curves for the different catalysts at varying scan rates for **b)** Ni_2P-Ru/NF, **c)** Ni_2P/NF, and **d)** bare NF.

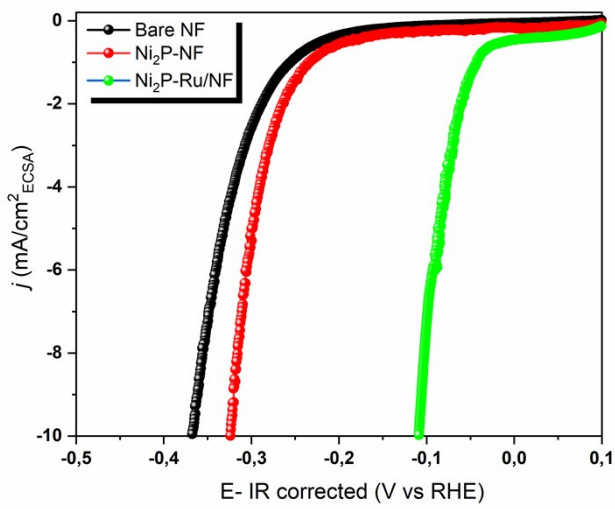

Figure S9. HER LSV curves normalized with ECSA for the Ni_2P-Ru/NF (24 h, 400 μm) along with bare NF (400 μm) and control sample of Ni_2P/NF (400 μm) in N_2-saturated 1 M KOH solution.

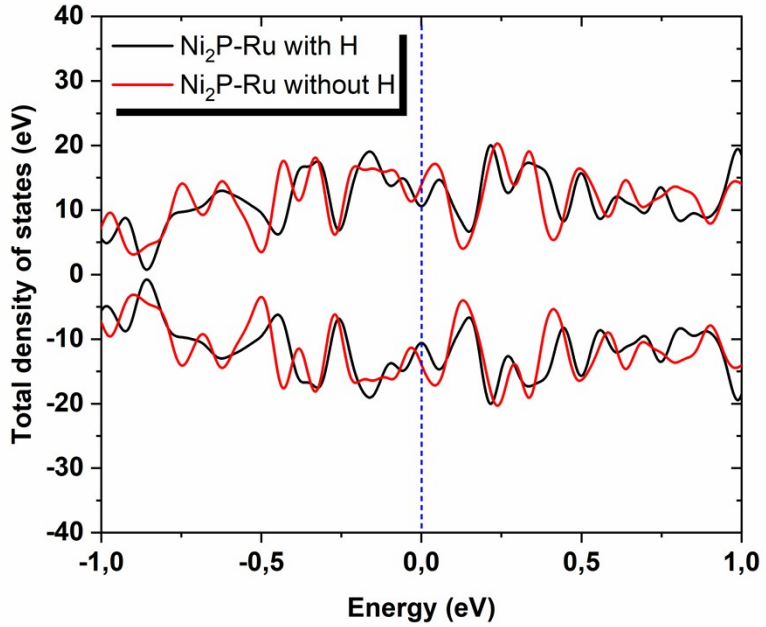

Figure S10. Total density of states (DOS) calculated for Ni_2P-Ru without and with H* adsorption (The values shown correspond to spin down and up states).

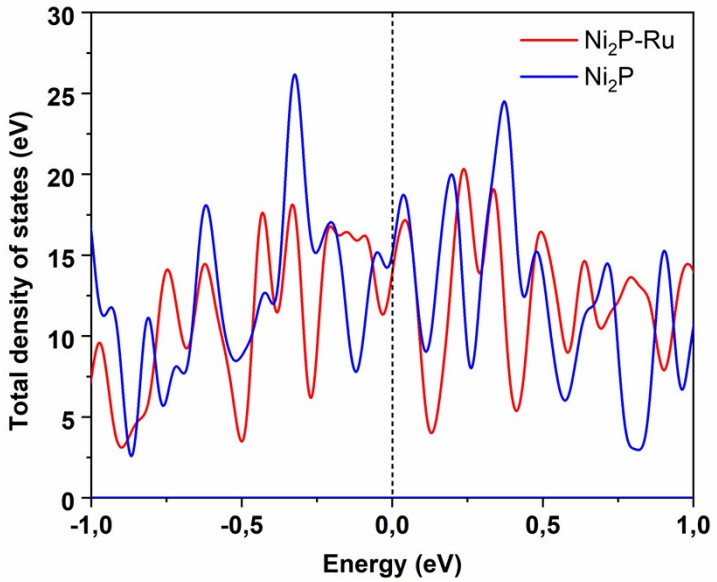

Figure S11. Total DOS calculated for Ni_2P and Ni_2P-Ru with the values shown corresponding to spin up states.

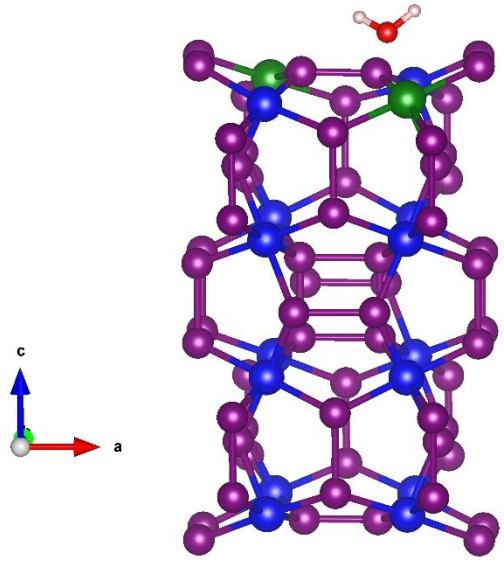

Figure S12. Optimized structure of Ni_2P-Ru after H_2O* adsorption.

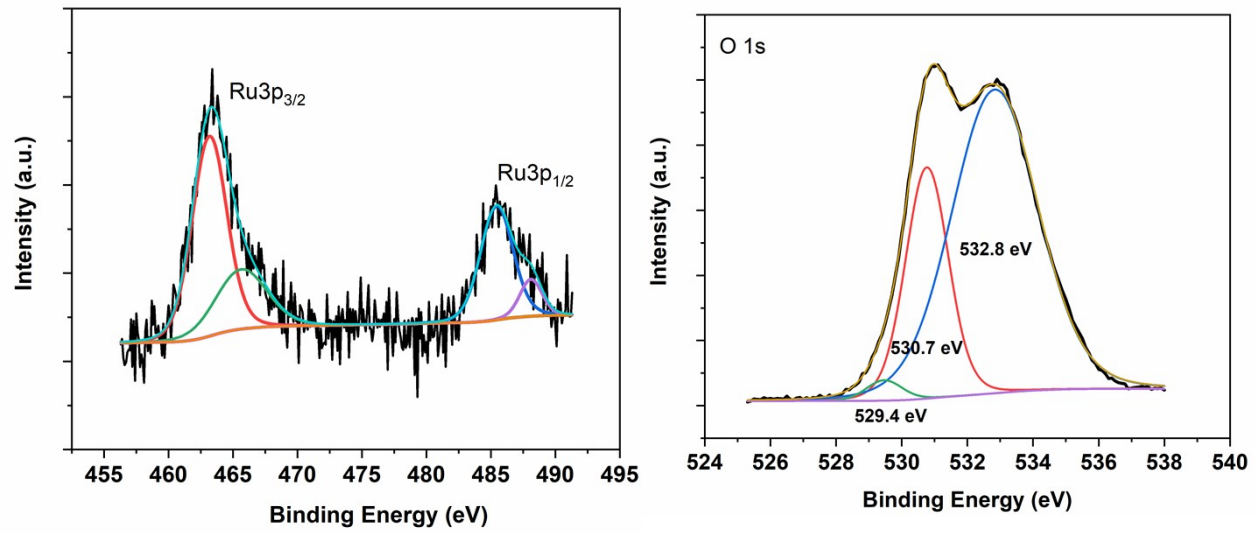

Figure S13. XPS deconvoluted spectra of **a)** Ru*3p* and **b**) O*1s* for Ni_2P-Ru/NF (24 h) after the HER durability test.

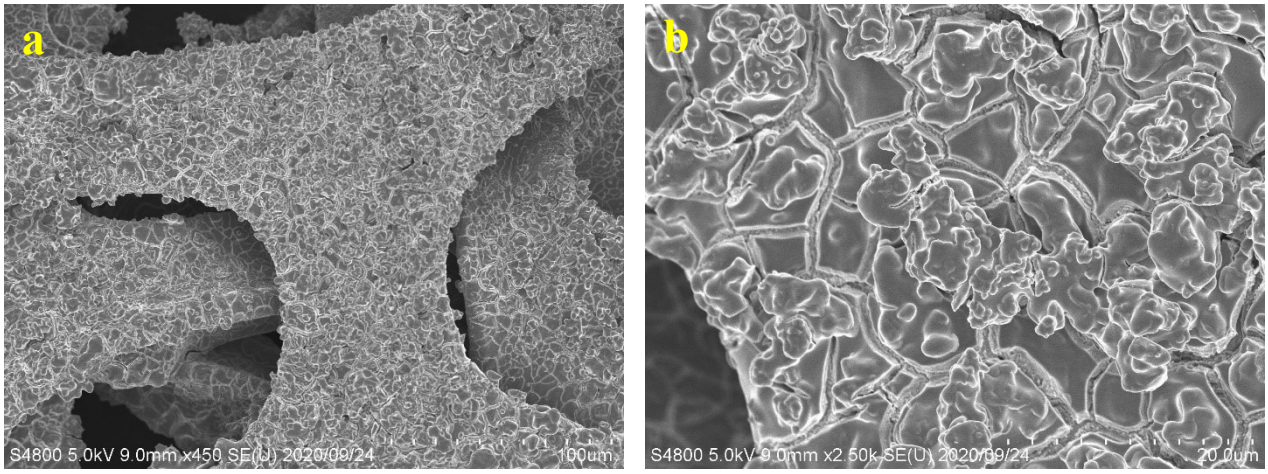

Figure S14. SEM images after the durability test for Ni_2P-Ru/NF (24 h).

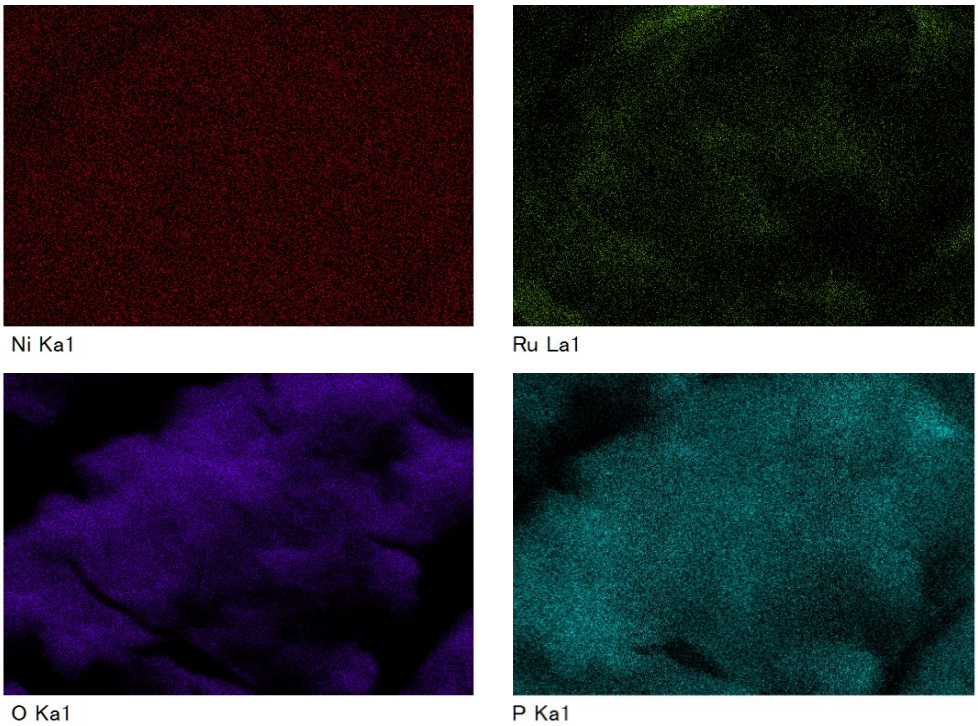

Figure S15. SEM-EDS mapping of Ni_2P-Ru/NF (24 h) after the durability test.

Table S4. The H* adsorption energy (ΔG_{H*} in eV) on different surfaces: Ru(001), N and P site of Ni_2P-Ru, Pt(111) site of Pt/C and PtRu/C, along with Ru site of PtRu/C. The distances (in Å) of interaction between hydrogen atom (H) and the different sites.

Configuration	Adsorption energy of H, ΔG_{H*} (eV)	H distance from surface (Å)
Ni_2P-H H on Ni	−1.28	Ni-H: 1.4846
Ni_2P-Ru-H H on Ru	0.128	Ru-H: 1.6528
Ni_2P-Ru-H H on Ni	0.425	Ni-H: 1.48
Ni_2P-Ru-H H on P	−0.131	P-H: 1.43
Pt (111)-C-H H on Pt	0.122	
Pt(111)-Ru-C-H H on Pt	−0.678	Pt-H: 1.88
Pt(111)-Ru-C-H H on Ru	−1.955	Ru-H: 1.66

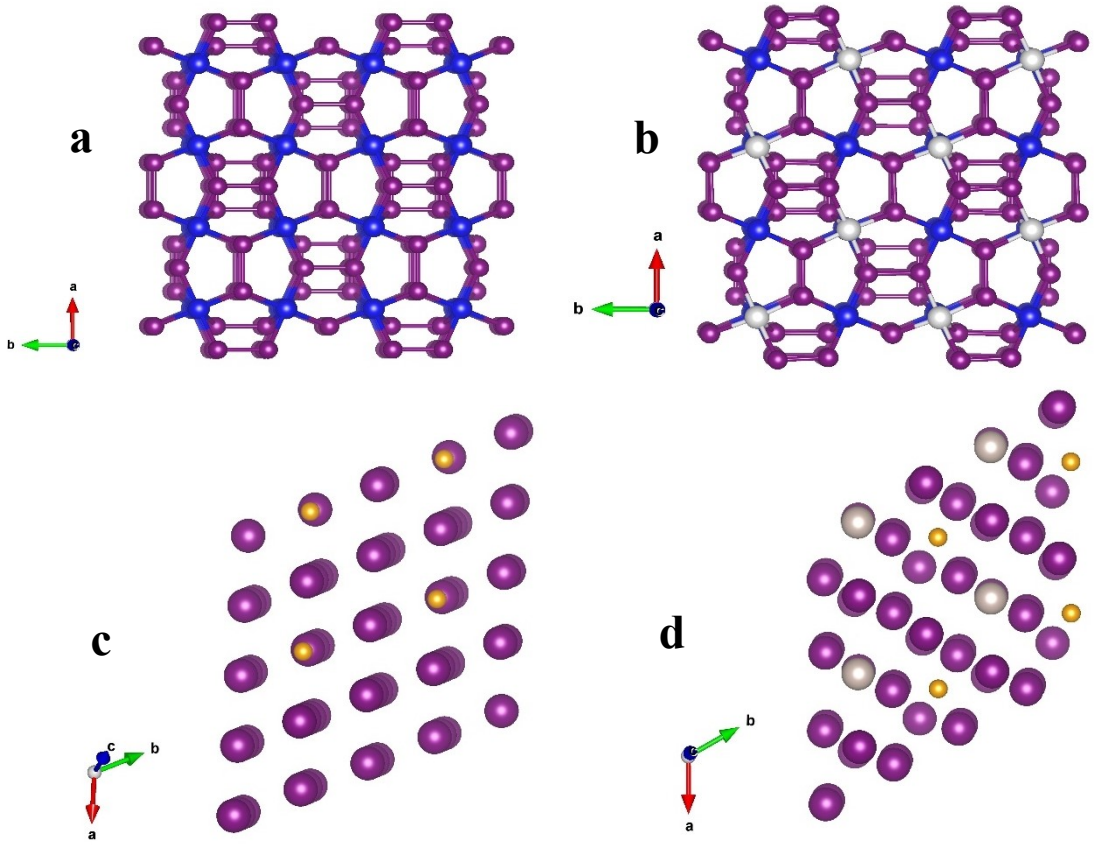

Figure S16. Modelled catalyst systems for the DFT studies: **a)** Ni_2P (*Purple : Ni, Blue : P*), **b)** Ni_2P-Ru (*Purple : Ni, Blue : P, Grey : Ru*), **c)** Pt/C ((*Purple : Pt, Yellow : C*), and **d)** PtRu/C (*Purple : Ni, Grey : Ru, Yellow : C)*.

Table S5. The H_2O* adsorption energy (eV) on different surfaces: Ru(001) site of Ni_2P-Ru, Pt(111) site of Pt/C. The distances (in Å) of interaction between surface and water molecule.

Configuration	Adsorption energy of H_2O (ΔG_{H_2O*}) (eV)	H_2O distance from surface (Å)
Ni_2P-Ru-H_2O H_2O on Ru	–0.458	2.3
Pt(111)-C-H_2O H_2O on Pt	1.15	3.5

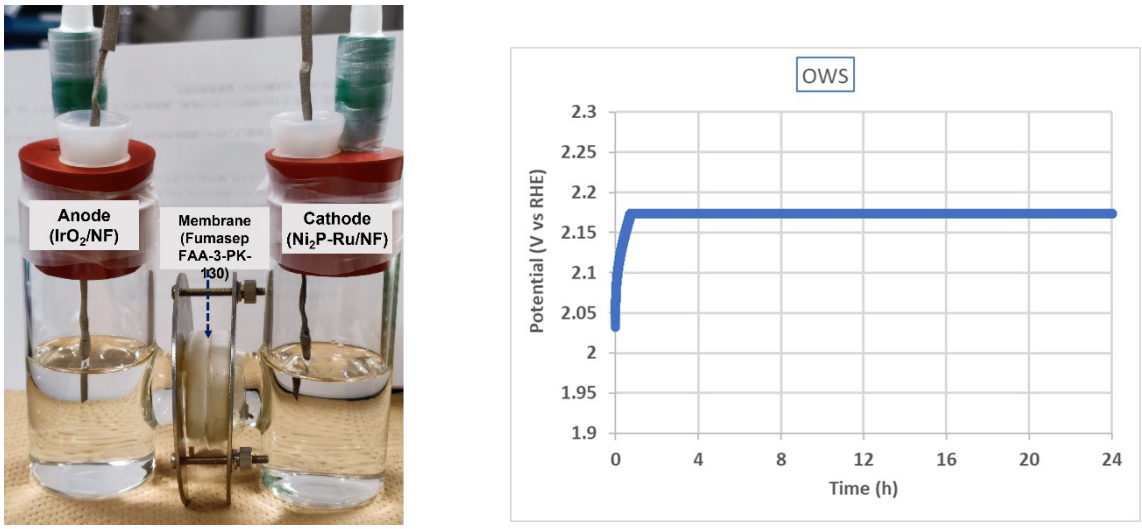

Figure S17 a) The H-type cell based overall water splitting (OWS) for qualitative assessment of the Ni_2P-Ru electrode **b)** Chronopotentiometry curve recorded for 24 h at 100 mA cm^{-2} showing the stability of the OWS system in 1M KOH solution.

References

1. C. Ling, H. Li, C. Yuan, Z. Yang, H. Chong, X. Qian, X. Lu, T. Cheang, A. Xu, Sulfur doped ruthenium nanoparticles as a highly efficient electrocatalyst for the hydrogen evolution reaction in alkaline media, ***Catal. Sci. Technol.***, 2021, **11**, 3865–3872.
2. Z. Pu, I. S. Amiinu, Z. Kou, W. Li, S. Mu, RuP_2-Based Catalysts with Platinum-like Activity and Higher Durability for the Hydrogen Evolution Reaction at All pH Values, ***Angew. Chem. Int. Ed.,*** 2017, 56, 11559.
3. J. Mahmood, F. Li, S. Jung, M. S. Okyay, I. Ahmad, S. Kim, N. Park, H. Y. Jeong, J. Baek, An efficient and pH-universal ruthenium-based catalyst for the hydrogen evolution reaction, ***Nat. Nanotech.,*** 2017,12, 441.
4. H. Chen, X. Ai, W. Liu, Z. Xie, W. Feng, W. Chen, X. Zo, Promoting Subordinate, Efficient Ruthenium Sites with Interstitial Silicon for Pt-Like Electrocatalytic Activity, ***Angew. Chem. Int. Ed.,*** 2019, 58, 11409.
5. Y. T. Li, F. Q. Chu, Y. F. Bu, Y. Kong, Y. X. Tao, X. Zhou, H. R. Yu, J. J. Yu, L. Tang, Y. Qin, Controllable fabrication of uniform ruthenium phosphide nanocrystals for the hydrogen evolution reaction, ***Chem. Commun***., 2019, 55, 7828–7831.

6. Z. Liu, Z. Li, J. Li, J. Xiong, S. Zhou, J. Liang, W. Cai, C. Wang, Z. Yang, H. Cheng, Engineering of Ru/Ru_2P interfaces superior to Pt active sites for catalysis of the alkaline hydrogen evolution reaction, ***J. Mater. Chem. A***, 2019, 7, 5621–5625.
7. Y. M. Zhao, X. W. Wang, G. Z. Cheng, W. Luo, Phosphorus induced activation of ruthenium for boosting hydrogen oxidation and evolution electrocatalysis, ***ACS Catal.,*** 2020, 10(20), 11751–11757.
8. X. Liu, F. Liu, J. Yu, G. Xiong, L. Zhao, Y. Sang, S. Zuo, J. Zhang, H. Liu, W. Zhou, Charge redistribution caused by S, P synergistically active Ru endows an ultrahigh hydrogen evolution activity of S-doped RuP embedded in N, P S-doped carbon, ***Adv. Sci.*** 2020, **7**(17), 2001526.
9. J. X. Guo, D. Y. Yan, K. W. Qiu, C. Mu, D. Jiao, H. Wang, T. Ling, High electrocatalytic hydrogen evolution activity on a coupled Ru and CoO hybrid electrocatalyst, ***J. Energy Chem***., 2019, 37, 143–147.
10. H. Song, M. Wu, Z. Tang, J. S. Tse, B. Yang, S. Lu, Single atom ruthenium-doped CoP/CDs nanosheets via splicing of carbon-dots for robust hydrogen production, ***Angew. Chem. Int. Ed.,*** 2021, 60(13), 7234–7244.
11. K. Wu, K. Sun, S. Liu, W. Cheong, Z. Chen, C. Zhang, Y. Pan, Y. Cheng, Z. Zhuang, X. Wei, Y. Wang, L. Zhang, Q. Zhang, D. Wang, Q. Peng, C. Chen, Y. Li, Atomically dispersed Ni–Ru–P interface sites for high-efficiency pH-universal electrocatalysis of hydrogen evolution, ***Nano Energy***, 2021, 80, 105467.
12. Y. Sun, Z. Xue, Q. Liu, Y. Jia, Y. Li, M. Liu, G. Li, C. Su, Modulating electronic structure of metal-organic frameworks by introducing atomically dispersed Ru for efficient hydrogen evolution, ***Nat. Commun***., 2021, 12(1), 1369.
13. P. Bhanja, B. Mohanty, S. Chongdar, A. Bhaumik, B. K. Jena, S. Basu, Novel Microporous Metal Phosphonates as Electrocatalyst for the Electrochemical Hydrogen Evolution Reaction, ***ACS Appl. Energy Mater.***, 2021, 4(11), 12827–12835.
14. Y. Qiu, M. Sun, J. Cheng, J. Sun, D. Sun, L. Zhang, Bifunctional Ni-Fe/$NiMoN_x$ nanosheets on Ni foam for high-efficiency and durable overall water splitting, ***Catal. Commun.***, 2022, 164, 106426.
15. J. Dong, Y. Wang, Q. Jiang, Z. Nan, F. R. Fan, Z. Tian, Charged droplet-driven fast formation of nickel–iron (oxy)hydroxides with rich oxygen defects for boosting overall water splitting, ***J. Mater. Chem. A***, 2021, 9, 20058–20067.
16. G. Ma, N. Yang, Y. Xue, G. Zhou, X. Wang, Ethylene Glycol Electrochemical Reforming Using Ruthenium Nanoparticle Decorated Nickel Phosphide Ultrathin Nanosheets, ***ACS Appl. Mater. Interfaces***, 2021, 13, 42763−42772.
17. Y. Yang, Q. Liu, H. Wang, H. Wen, Z. Peng, K. Xiang, C. Gao, X. Wu, B. Li, Z. Liu, Phosphorus-Doped 3D RuCo Nanowire Arrays on Nickel Foam with Enhanced Electrocatalytic Activity for Overall Water Splitting, ***ACS Omega***, 2021, 6, 10234−10241.
18. H. Wang, H. Liu, T. Feng, L. Wang, W. Yuan, Q. Huang, Y. Guo, Electronically modulated nickel boron by CeO_x doping as a highly efficient electrocatalyst towards overall water splitting, ***Dalton Trans.***, 2022, 51, 675−684.
19. L. Li, Y. Lu, X. Liu, X. Wang, S. Zhou, Layered double hydroxide drived ultra-evenly Rh-doped Co_2Fe-P composite for high-efficient overall water splitting, ***J. Alloys and Comp***., 2022, 895, 1625492.
20. Y. Peng, H. He, Novel heterostructure Cu_2S/Ni_3S_2 coral-like nanoarrays on Ni foam to enhance hydrogen evolution reaction in alkaline media, ***RSC Adv***., 2021, 11, 39493−39502.
21. Y. Dong, H. Su, G. Liu, Exploring the electrocatalytic activity of cobalt disulfide nanosheets towards the hydrogen evolution reaction with *in situ* ECAFM, ***Sustainable Energy Fuels***, 2021, 5, 4115−4125.

22. S. C. Karthikeyan, R. S. Kumar, S. Ramakrishnan, S. Prabhakaran, A. R. Kim, D. H. Kim, D. J. Yoo, Efficient Alkaline Water/Seawater Electrolysis by Development of Ultra-Low IrO_2 Nanoparticles Decorated on Hierarchical MnO_2/rGO Nanostructure, ***ACS Sustainable Chem. Eng***., 2022, 10, 15068−15081.
23. S. Li, C. Xi, Y. Z. Jin, D. Wu, J. Q. Wang, T. Liu, H. B. Wang, C. K. Dong, H. Liu, S. A. Kulinich, X. W. Du, Ir-O-V Catalytic Group in Ir-Doped $NiV(OH)_2$ for Overall Water Splitting, ***ACS Energy Lett.***, 2019, 4(8), 1823–1829.
24. F. Lv, W. Zhang, W. Yang, J. Feng, K. Wang, J. Zhou, P. Zhou, S. Guo, Ir-Based Alloy Nanoflowers with Optimized Hydrogen Binding Energy as Bifunctional Electrocatalysts for Overall Water Splitting, ***Small Methods***, 2020, 4(6), 1–7.
25. N. Chen, Y. Du, G. Zhang, W. Lu, F. Cao, Amorphous nickel sulfoselenide for efficient electrochemical urea-assisted hydrogen production in alkaline media, ***Nano Energy***, 81, 2021, 105605.
26. S. Riyajuddin, K. Azmi, M. Pahuja, S. Kumar, T. Maruyama, C. Bera, K. Ghosh, Super-Hydrophilic Hierarchical Ni-Foam-Graphene-Carbon Nanotubes-Ni_2P–CuP_2 Nano-Architecture as Efficient Electrocatalyst for Overall Water Splitting, ***ACS Nano***, 2021, 15(3), 5586–5599.
27. J. Dong, Y. Wang, Q. Jiang, Z. Nan, F. R. Fan, Z. Tian, Charged droplet-driven fast formation of nickel–iron (oxy)hydroxides with rich oxygen defects for boosting overall water splitting, ***J. Mater. Chem. A***, 2021, 9, 20058–20067.
28. N. K. Oh, J. Seo, S. Lee, H. Kim, U. Kim, J. Lee, Y. Han, H. Park, Highly efficient and robust noble-metal free bifunctional water electrolysis catalyst achieved via complementary charge transfer, ***Nat. Commun***., 2021, 12, 4606.
29. W. Lai, L. Zhang, W. Hua, S. Indris, Z. Yan, Z. Hu, B. Zhang, Y. Liu, L. Wang, M. Liu, R. Liu, Y. Wang, J. Wang, Z. Hu, H. Liu, S. Chou, S. Dou, General π-Electron-Assisted Strategy for Ir, Pt, Ru, Pd, Fe, Ni Single-Atom Electrocatalysts with Bifunctional Active Sites for Highly Efficient Water Splitting, ***Angew. Chem. Int. Ed.***, 2019, 58(34), 11868–11873.
30. C. Wang, F. Wang, S. Qiu, J. Gao, L. Gu, K. Wang, P. Zuo, K. Sun, X. Zhu, Integrating Co_3O_4 Nanoparticles with MnO_2 Nanosheets as Bifunctional Electrocatalysts for Water Splitting, ***Int. J. Hydrogen Energy***, 2021, 46(17), 10356–10365.
31. H. Zhang, X. Wu, C. Chen, C. Lv, H. Liu, Y. Lv, J. Guo, J. Li, D. Jia, F. Tong, Spontaneous ruthenium doping in hierarchical flower-like Ni_2P/NiO heterostructure nanosheets for superb alkaline hydrogen evolution, ***Chem. Eng. J.***, 2021, 417, 128069.